

STATIC CONTROL OF DRAG-REDUCING AIR CAVITIES WITH VARIABLE CAVITATOR SHAPE

(DOI No: 10.3940/rina.ijme.2019.a1.516)

K I Matveev, Washington State University, USA

SUMMARY

Air ventilation of submerged surfaces of ship hulls is a promising technique for drag reduction. To ensure high performance of air cavities in a broad range of operational conditions, the cavity properties can be controlled with help of compact hydrodynamic actuators. In this study, a potential flow theory is applied to model an air cavity formed behind a wedge-shaped cavitator under a horizontal wall imitating a ship bottom. By varying the wedge angle, it is possible to achieve states with maximum drag reduction at given operational conditions. The dependence of the optimal wedge angle on Froude number and hull trim is investigated. The air-cavity ability to reduce frictional drag is found to increase with rising flow speed and bow-down hull trim.

NOMENCLATURE

c	Cavitator length (m)
C_f	Friction coefficient
C_p	Pressure coefficient
D_w	Wedge pressure drag (N)
ΔD_f	Frictional drag reduction (N)
Fr	Froude number based on cavitator length
g	Gravity constant (m s^{-2})
L_c	Air-cavity length (m)
L_e	Equivalent drag-free length (m)
p_0	Upstream flow pressure (Pa)
p_c	Air-cavity pressure (Pa)
q	Hydrodynamic source intensity ($\text{m}^2 \text{s}^{-1}$)
u_0	Incident flow velocity (m s^{-1})
u_c	Flow velocity on the cavity boundary streamline (m s^{-1})
u'	Velocity perturbation (m s^{-1})
x^c	Horizontal position of a collocation point (m)
x^s	Horizontal position of a source (m)
Δx	Distance between sources (m)
y_c	Vertical coordinate of the cavity boundary (m)
y_w	Vertical coordinate of the wedge cavitator (m)
α	Cavitator angle (deg or rad)
β	Performance coefficient of the wedge-cavity system
η	Efficiency of the wedge-cavity system
ρ	Density of water (kg m^{-3})
σ	Cavitation number
τ	Trim angle (deg or rad)

1. INTRODUCTION

Conserving energy and reducing environmental impacts are two major goals of modern engineering developments, including ship design. The world fleet of marine vessels is one of the main consumers of fossil fuels and contributors to pollutant emission. Significantly reducing hydrodynamic resistance of ships can decrease energy consumption and pollution. However, traditional ship hulls are already optimized to the point where small modifications of hull forms do not produce a significant benefit. Advanced marine vehicles with radically

different hulls (such as hydrofoils, air cushion vehicles, and multi-hulls) have found niche applications, but their limited payload capabilities and high cost have prevented their broader use as oceanic transports.

One of the most promising radical techniques for water drag reduction involves air-ventilated cavities formed on underwater surfaces of ship hulls. Examples of possible implementations (among others) of this idea on displacement hulls are shown in Figure 1. Reduction of the hull wetted area by air cavities can decrease drag by 10-25% (Matveev, 2005; Makiharju *et al.*, 2012). Although this technique was studied in the past and several prototype boats were built (some with questionable success), the widespread implementation has not yet occurred. The primary reason is insufficient understanding of how to maintain stable large-area air cavities at small air supply rates in a wide range of operational conditions, including off-design loading/speed regimes and sailing in waves.

In this work, a shape of the wedge cavitator (behind which an air cavity is produced) is considered as a controlled parameter. Using an idealized mathematical model in a simple two-dimensional setting, it is shown how an optimal value for the wedge angle can be selected to optimize drag-reducing performance of the air-cavity setup. The problem analysed here is static with no time-dependent variations of the flow or cavitator shape. More general problem of dynamic control of air cavities was recently discussed by Amromin (2015).

The mathematical framework utilized in this study is based on the potential flow theory and modelling methods previously applied and validated for surface flows around a variety of air-assisted and planing hulls, including those with fixed air-cavity systems (Matveev, 2003; Matveev & Ockfen, 2009; Matveev, 2014; Matveev, 2015). For additional information on the air-ventilated drag reduction technology, the readers can refer to publications on the air-cavity flow physics (Ceccio, 2010), laboratory experiments (Arndt *et al.*, 2009; Lay *et al.*, 2010; Matveev *et al.*, 2009; Makiharju *et al.*, 2013; Zverkhovskiy *et al.*, 2014, Butterworth *et al.*, 2015), modelling methods (Choi & Chahine, 2010; Shiri *et al.*, 2012; De Marco *et al.*, 2017),

and practical developments (Latorre, 1997; Matveev *et al.*, 2006; Dize, 2007; Kawakita *et al.*, 2015).

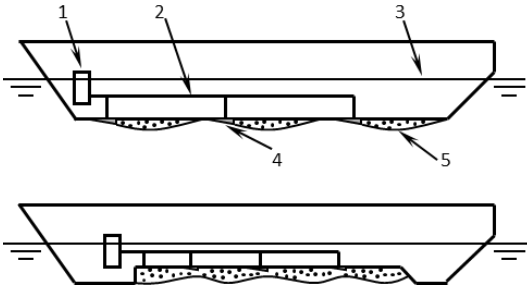


Figure 1. Displacement vessels with air-cavity systems: top, with several cavities; bottom, with single multi-wave cavity. 1, air blower; 2, air pipeline; 3, free water surface; 4, cavitator; 5, air cavity.

2. MATHEMATICAL MODEL

A schematic of water flow under horizontal wall with an air cavity formed behind a wedge-shaped cavitator with length c and small angle α is given in Figure 2. The water flow is considered to be two-dimensional, steady, irrotational, incompressible and inviscid. Far upstream and downstream the water flow is uniform and parallel to the wall, which imitates the ship bottom. The gravity is accounted for, and for cases with a trimmed hull the gravity vector forms a small angle τ with the y -axis. The air cavity is assumed to attach to the wall at a distance L_c (cavity length) from the wedge without forming a forward water jet or producing shed air bubbles. This model works well for developed cavitating/ventilated flows in case of long and stable gaseous cavities (Knapp, 1970). The pressure inside the air cavity, p_c , is related to the pressure the upstream flow, p_0 , via a cavitation number,

$$\sigma = \frac{p_0 - p_c}{\frac{1}{2}\rho u_0^2}, \quad (1)$$

where ρ is the water density and u_0 is the upstream flow velocity.

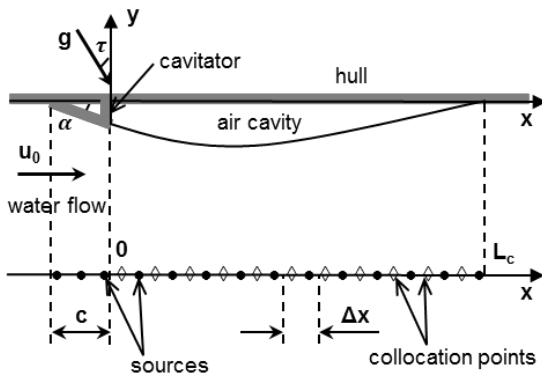


Figure 2. Top, model for air cavity formed behind wedge cavitator. Bottom, positioning of sources and collocation points along the hull bottom (x -axis). Sources are shown by filled circles; collocation points are given by diamonds. Distances between sources (Δx) is exaggerated.

The air cavity shape can be determined from the boundary conditions of the cavity boundary. The dynamic condition follows from the Bernoulli equation that can be written for the cavity surface streamline as follows,

$$p_0 + \frac{1}{2}\rho u_0^2 = p_c + \frac{1}{2}\rho u_c^2 + \rho g(y_c - x \sin \tau), \quad (2)$$

where y_c and u_c are the vertical coordinate and the water flow velocity at the cavity boundary, x is the coordinate along the wall, τ is the trim angle in radians, and g is the gravity constant. A linearized formulation is considered in this study implying that slopes of the water surface are small. Then, a linear form of the Bernoulli equation can be used on the cavity surface,

$$\frac{\sigma}{2} = \frac{u'}{u_0} + \frac{gy_c}{u_0^2}, \quad (3)$$

where $u' = u - u_0$ is the perturbed water flow velocity. On the wetted surface of the wedge, an equation similar to Eq. (2) can be applied, but instead of the cavitation number one needs to use an x -dependent pressure coefficient,

$$-\frac{C_p}{2} = \frac{u'}{u_0} + \frac{gy_w}{u_0^2}. \quad (4)$$

where $C_p = (p - p_0)/(0.5\rho u_0^2)$ is the pressure coefficient and y_w is the vertical coordinate of the wedge sloping surface. The solution for the water flow around the cavitator with an air cavity can be found by distributing hydrodynamic point sources along the wall surface at $y = 0$ (Figure 2). The boundary conditions are satisfied at the collocation points that are shifted forward with respect to the sources in order to minimize effect of the downstream boundary (Bertram, 2000). The horizontal velocity disturbance can be computed by adding contributions from all sources,

$$u'(x_i^c) = \frac{1}{2\pi} \sum_j \frac{q_j}{x_i^c - x_j^s}, \quad (5)$$

where x_i^c and x_j^s are horizontal locations of the i -th collocation point and the j -th source with strength q_j .

The linear kinematic boundary condition on the free surface implies that the intensity of local sources is proportional to the surface slope (Katz & Plotkin, 2001; Matveev & Ockfen, 2009),

$$\frac{q_i + q_{i-1}}{2\Delta x} = -2u_0 \frac{y_i^s - y_{i-1}^s}{\Delta x}, \quad (6)$$

where Δx is the numerical cell length and y_i^s is the water surface elevation at the i -th source location. On the cavitator surface, this elevation is known, and therefore, the source strengths at $x < 0$ can be related to the given wedge angle, $q_i = 2u_0 \alpha \Delta x$, where α is in radians.

Besides the kinematic and dynamic boundary conditions, additional matching conditions ensure that the cavity surface slope near the cavitator equals to the wedge angle and that the cavity tail attaches to the wall at $x = L_c$.

For a set of given parameters, which include the wedge-length Froude number $Fr = u_0/\sqrt{gc}$, wedge angle α , hull trim τ , and cavity length L_c , a system of linear equations can be formed using the above equations. The unknown variables include the air cavity ordinates, the source intensities on the cavity surface, and the cavitation number. This system of equations is solved directly.

However, in the analysis below the cavitation number σ is treated as a given input, whereas the cavity length L_c is an outcome of calculations. Hence, in order to determine the cavity length, the first step in this study was to establish dependence $\sigma(L_c)$ for a specified set of other parameters (Fr, α, τ). Then, using a given input value of σ , the cavity length was found by interpolation from the obtained correlation between σ and L_c .

The adequate number of sources (and collocation points) that need to be placed along the cavity is determined from mesh-dependency studies. For the calculation cases considered below, it was established that the distance between source can be chosen in relation to the cavitator length as $\Delta x = c/80$.

Upon finding the cavity shape and the source intensities, the pressure coefficient on the wetted cavitator surface can be calculated with Eq. (4). Accounting for air-cavity pressure with help of cavitation number, and the wedge pressure drag in the two-dimensional flow can be computed as follows,

$$D_w = \frac{1}{2} \rho u_0^2 (\bar{C}_p + \sigma) \alpha c. \quad (7)$$

where \bar{C}_p is the average pressure coefficient on the cavitator wetted surface.

The main purpose of the air cavity is to reduce water friction of the ship hull surface. In the present formulation, the frictional drag reduction can be related to a decrease of the hull wetted surface,

$$\Delta D_f = \frac{1}{2} \rho u_0^2 C_f L_c, \quad (8)$$

where C_f is the effective friction coefficient. Combining the frictional drag reduction and the cavitator pressure drag, an equivalent drag-free length, L_e , can be introduced as follows,

$$\frac{L_e}{c} = \frac{L_c}{c} - \frac{\bar{C}_p + \sigma}{C_f} \alpha. \quad (9)$$

As one can see from Eq. (9), the equivalent drag-free length will be smaller than the air cavity length. An idealized drag-reducing efficiency of the wedge-cavity

system can be defined for characterizing the effectiveness of the hull area utilization,

$$\eta = \frac{L_e}{c + L_c}. \quad (10)$$

In cases when the maximum cavity length is limited to some given length L_0 (e.g., due to downstream presence of another cavitator or a curved hull section), the performance coefficient β can be used,

$$\beta = \frac{L_e}{c + L_0}. \quad (11)$$

It should be noted that there are additional factors that may decrease the actual air-cavity efficiency. For example, extra power needs to be spent for supplying air into the cavity. Also, if the cavity pressure is lower than the upstream water flow pressure at the hull bottom, then a sinkage of the entire ship hull may increase, and this will lead to some additional drag. These factors would need to be included when designing an actual air-cavity ship with a specified hull form. However, in the present formulation both the air leakage from the cavity and the ship sinkage are ignored.

3. RESULTS

One example of the present method validation is given in Figure 3 for the length of an air cavity formed under a two-dimensional hull form tested in a recirculating water channel (Matveev *et al.*, 2009). The hull length and beam of the experimental model were about 56 cm and 31 cm, respectively. The tested conditions included hull drafts of 1.3 cm and 4.1 cm at zero trim, whereas the incident flow velocities ranged between 28 cm/s and 86 cm/s. The air cavity was generated in experiments by supplying a minimum amount of air (about 0.8 standard cubic cm per second) needed to maintain an elongated air cavity behind the step in a steady water flow. The total experimental uncertainties are included in Figure 3 as error bars. A good agreement between numerical and experimental results in Figure 3 indicates the ability of the potential-flow model to adequately predict the air-cavity shape.

The main goal of this study is to illustrate how optimal angles of a cavitator under the wall imitating a ship bottom (Figure 2) can be selected in given operational conditions. The default condition was chosen with zero trim of the wall and Froude number $Fr = u_0/\sqrt{gc} = 2.5$. The pressure inside air cavities on displacement ships is usually slightly lower than the pressure in the water flow at the bottom level. In this study, the cavitation number is treated as a given fixed input parameter, $\sigma = 0.05$. In order to find the cavity shape and length, corresponding to this σ , a set of different cavity lengths are tried in initial calculations, and then the results are interpolated to determine the cavity length L_c for the given σ . The variable parameter in the first series of calculations was the cavitator angle α . This

problem formulation corresponds to a practical situation when the cavitator angle can be controlled, for example, with mechanical actuators.

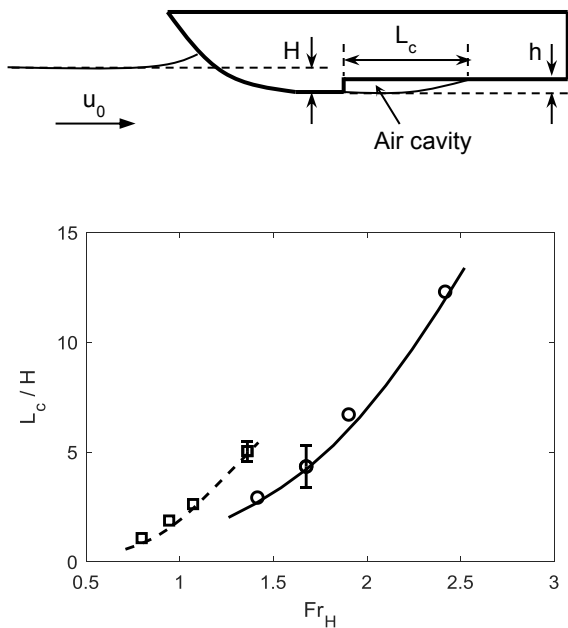


Figure 3. Top, schematic of experimental hull. Bottom, comparison of modelling results (curves) and test data (symbols). Circles and solid curve correspond to submergence-to-step height ratio $H/h = 1.4$; squares and dashed curve to $H/h = 4.3$. Error bars indicate experimental uncertainties.

The computed length of the air cavity, the equivalent “drag-free” length and the cavity efficiency are shown in Figure 4 as functions of the wedge angle. In the considered condition the cavity length increases from about 2.5 of the cavitator length to about $5.5c$ as the cavitator angle increases from 2 to 5 degrees. The equivalent length also becomes longer, but it remains smaller than the cavity length due to the wedge pressure drag; and the rate of growth of L_e decreases at higher wedge angles. Hence, even if the frictional drag reduction is higher at longer L_c , the pressure drag may reduce the air-cavity effectiveness. This is reflected in the efficiency plot in Figure. 4, where η exhibits a maximum, close to 60%, at the optimal cavitator angle of about 3.2° . The cavity length at this point is about $4c$.

Taking $Fr = 2.5$ and $\tau = 0^\circ$ as the most common (cruise) condition for a hypothetical ship in the present analysis, a system of similar cavitators can be chosen on the hull bottom so that lengths available for air cavities behind each cavitator will correspond to the optimal value found above ($L_0 \approx 4c$). This cruise condition, although most frequent, may not be always feasible. For example, the ship may have to sail at other speeds in specific environmental conditions and have a non-zero trim due to non-optimal cargo loading. Hence, cavitators with a fixed angle are unlikely to achieve the highest

drag-reducing potential in such situations. It can be expected, however, that by controlling the cavitator angles one can improve the air-cavity performance in off-design sailing regimes.

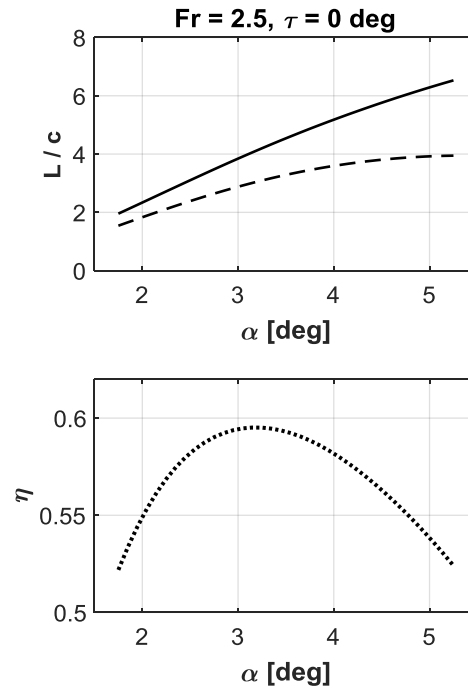


Figure 4. Air-cavity length (solid line), equivalent length (dashed line), and air-cavity efficiency (dotted line) at $Fr = 2.5$ and zero trim.

The second set of calculations has been conducted here for a range of hull speeds (or Froude numbers) keeping the zero hull trim. Results for additional four Fr ranging from 2 to 3 are shown in Figure 5. The cavity length and the equivalent drag-free length increase with the cavitator angle as for the previous case with $Fr = 2.5$, and the length values also increase at higher speeds, which is a well-known effect in air-ventilated/cavitating flows. The cavity efficiencies η grow with Froude numbers as well, and their maxima shift to higher cavitator angles α . However, not all of these values are achievable now, since a restriction is put in place for the maximum possible cavity length ($L_0 \approx 4c$) selected above from the most optimal case at $Fr = 2.5$ and $\tau = 0^\circ$. With the cavity length limited to L_0 , it is more appropriate to use the performance coefficient β , defined by Eq. (11). In Figure 5, the optimal values for β are also shown, corresponding to intersections of β and η curves, since that is when the cavity length reaches L_0 .

Results for the optimal cavitator angle and highest possible performance coefficients at various Froude numbers are summarized in Figure 6. The cavitator angle α decreases with increasing Fr , since it is easier to form longer cavities at higher flow speeds. The drag-reducing performance improves at higher Fr due to lower pressure drag of cavitators with smaller angles.

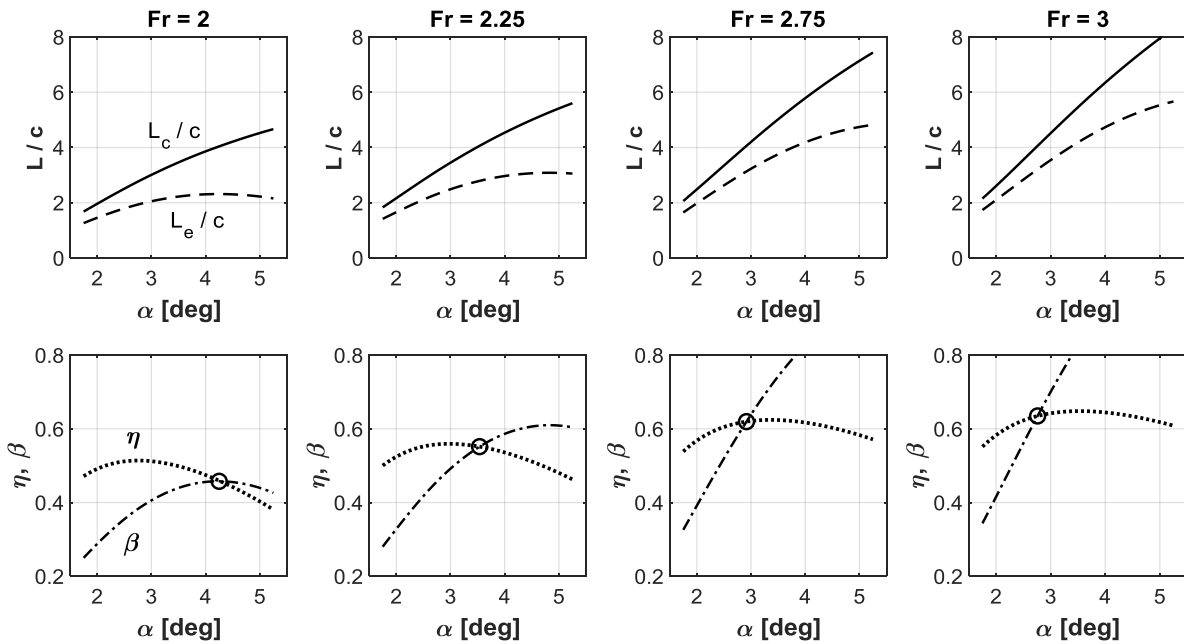


Figure 5. Air-cavity length (solid line), equivalent length (dashed line), air-cavity efficiency (dotted line), and performance coefficient (dash-dotted line) at variable cavitation angles and several Froude numbers. Circles indicate highest possible β .

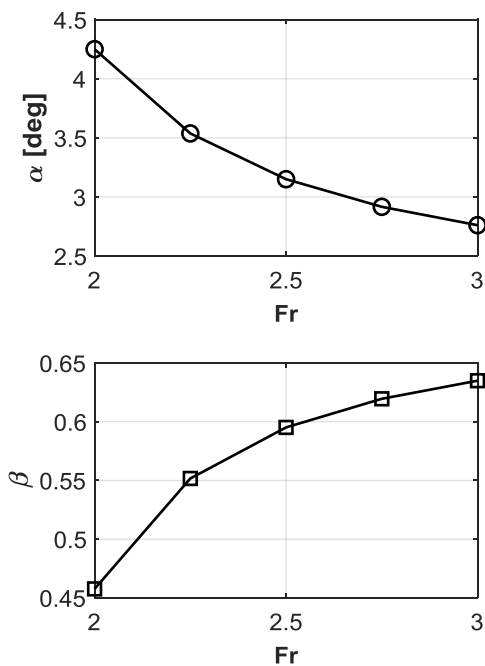


Figure 6. Optimal cavitation angle (circles) and corresponding air-cavity performance coefficient (squares) at variable Froude numbers and zero trim.

A comment needs to be added here concerning the most efficient cavitation deployment on ships operating in a broad range of speeds (this is particularly important for fast ships and boats). Since longer cavities can be produced at higher speeds, it may be possible to generate a sufficiently long cavity by a single cavitation that will cover the length of two short cavities formed by two

cavitation (Figure 7); the second cavitation can be retracted to the hull bottom in this case. The present example indicates that this can be possible at $Fr = 3$ and cavitation angle around $5-6^\circ$ (slightly beyond the studied range). Such an option may be especially attractive if the gas leakage from one long cavity is substantially smaller than the combined leakage from two shorter cavities. However, a detailed analysis of this effect is beyond the present model in which the air leakage is not considered.

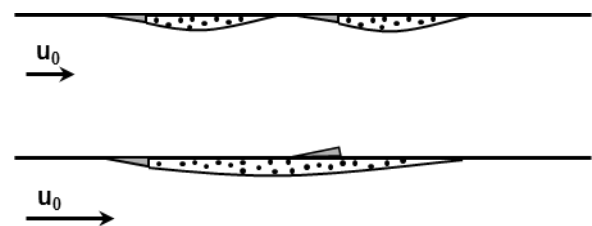


Figure 7. Illustrations of two short cavities at low speed (top) and a single long cavity at high speed (bottom). The second cavitation is retracted into the hull at higher speed.

As another calculation example of varying operational conditions, a set of non-zero hull trims ($\pm 2^\circ$) is considered here at the default Froude number of 2.5. The results for the cavity lengths, equivalent lengths, efficiencies and performance coefficients are shown in Figure 8. The characteristic lengths again increase at higher cavitation angle, but they decrease as the wall trim changes from negative (bow-down) to positive (bow-up) values. The reason is that the air in the cavity will

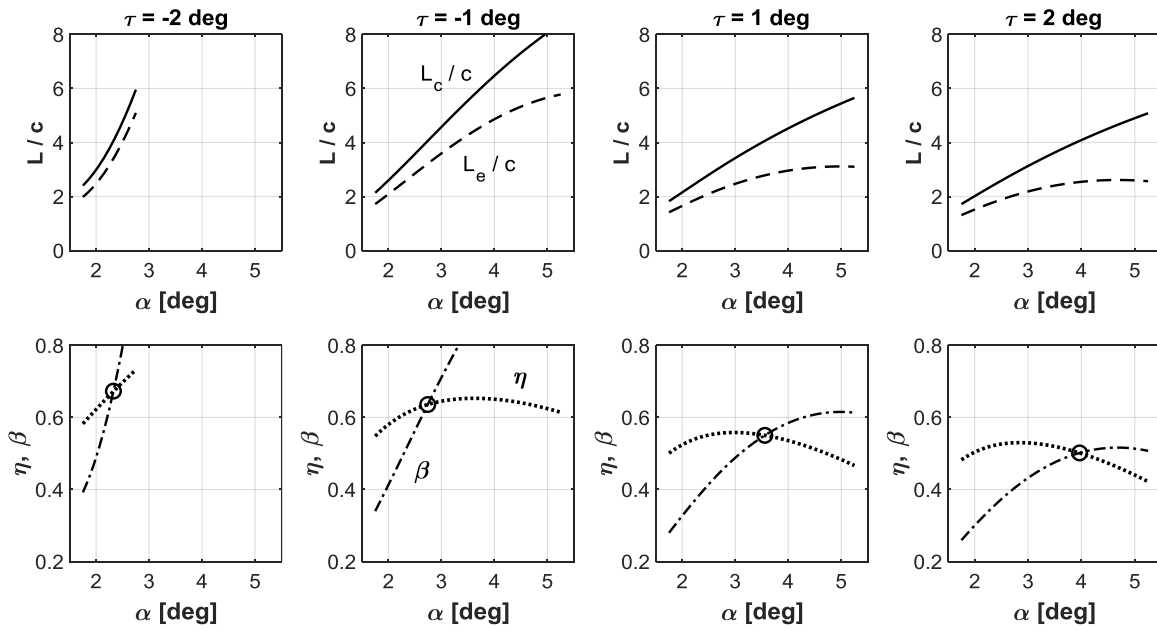


Figure 8 Air-cavity length (solid line), equivalent length (dashed line), air-cavity efficiency (dotted line), and performance coefficient (dash-dotted line) at variable cavitator angles and several trim angles. Circles indicate highest possible β .

propagate more easily in the upward direction behind the wedge due to buoyancy. With the negative trim -2° , the air cavity reaches the limited value L_0 already at about $\alpha = 2.3^\circ$, while it takes $\alpha = 4^\circ$ to reach the same limit at positive trim $+2^\circ$. Again, the intersections of curves for η and β define the most favourable operational points under the cavity length restriction.

The optimal cavitator angles and performance coefficients are plotted in Figure 9 as a function of the wall trim. With larger bow-up trim, α values increase almost linearly, while β values decrease. It should be noted that although a bow-down hull trim is more favourable for the air cavities, the ship wave resistance may increase. When designing an air-cavity ship, all factors affecting the total hull drag must be taken into account.

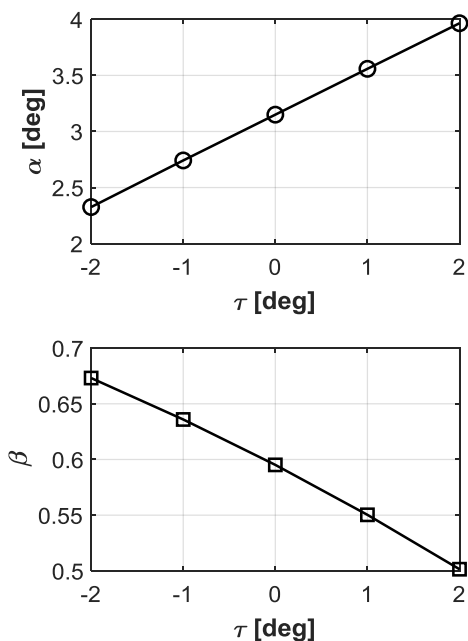


Figure 9. Optimal cavitator angle (circles) and corresponding air-cavity performance coefficient (squares) at variable trim angles and $Fr = 2.5$.

Another note can be made about possible three-dimensional effects. The air cavities restricted from the sides with plates or placed in recesses on hull bottoms often exhibit elongations at their lateral boundaries in comparison with the centreline portions. Since a length of a thin cavity generally increases with the wedge angle, it may be beneficial to reduce the cavitator angle near the sides in order to keep the air cavity length more uniform. For more confident analysis of such effects, three-dimensional modelling is needed (e.g., Matveev, 2015).

4. CONCLUSIONS

In the present potential-flow analysis, it is demonstrated how the drag-reducing performance of air-ventilated cavities can be statically controlled and optimized with help of variable-shape cavitators. Specifically, it is shown that there exists an optimal angle of the wedge cavitator maximizing drag reduction per area occupied by the cavitator-and-cavity system. With variation of the hull speed and trim, the cavitator angle needs to be varied to achieve the highest performance in new conditions. In

general, the air-cavity potential for frictional drag reduction increases at higher speed and negative (bow-down) trim.

Given a number of simplifying assumptions used in this study, the presented results should be treated as qualitative indicators of trends in the expected air-cavity performance. For more accurate predictions and optimization of more complex air-cavity systems on actual ships, the present theory can be used as guidance when conducting experimental tests and applying more expensive computational fluid dynamics tools that account for viscous, nonlinear and other phenomena ignored in the present formulation.

5. ACKNOWLEDGEMENTS

This material is based upon research supported by the National Science Foundation under Grant No. 1800135.

6. REFERENCES

- AMROMIN, E. (2015) *Ships with ventilated cavitation in seaways and active flow control*. Applied Ocean Research, 50, 163-172.
- ARNDT, R.E.A., HAMBELTON, W.T., KAWAKAMI, E., and AMROMIN, E.L. (2009) *Creation and maintenance of cavities under horizontal surfaces in steady and gust flows*. Journal of Fluids Engineering, 131, 111301-1.
- BERTRAM, V. (2000) *Practical Ship Hydrodynamics*. Butterworth-Heinemann, Oxford, UK.
- BUTTERWORTH, J., ATLAR, M., and SHI, W. (2015) *Experimental analysis of an air cavity concept applied on a ship hull to improve the hull resistance*. Ocean Engineering, 110, 2-10.
- CECCIO, S.L. (2010) *Friction drag reduction of external flows with bubble and gas injection*. Annual Review of Fluid Mechanics, 42, 183-203.
- CHOI, J.-K. and Chahine, L. (2010) *Numerical study on the behaviour of air layers used for drag reduction*. 28th Symposium on Naval Hydrodynamics, Pasadena, California, USA.
- DE MARCO, A., MANCINI, S., MIRANDA, S., SCOGNAMIGLIO, R., and VITIELLO, L. (2017) *Experimental and numerical analysis of a stepped planing hull*. Applied Ocean Research, 64, 135-154.
- DIZE, A.P. (2007) *Quadrapod air-assisted catamaran hull*. 1st Chesapeake Power Boat Symposium, Annapolis, MD.
- KNAPP, R.T., DAILY, J.W., and HAMMIT, F.G. (1970) *Cavitation*. McGraw-Hill, New York, USA.
- LATORRE, R. (1997) *Ship hull drag reduction using bottom air injection*. Ocean Engineering, 24, 161-175.
- LAY, K.A., YAKUSHIJI, R., MAKIHARJU, S., PERLIN, M., and CECCIO, S.L. (2010) *Partial cavity drag reduction at high Reynolds numbers*. Journal of Ship Research, 54, 109-119.
- KATZ, J. and PLOTKIN, A. (2001) *Low-Speed Aerodynamics*. Cambridge University Press, Cambridge, UK.
- KAWAKITA, C., SATO, S., and OKIMOTO, T. (2015) *Application of simulation technology to Mitsubishi air lubrication system*. Mitsubishi Heavy Industries Technical Review, 52(1), 50-56.
- MAKIHARJU, S.A., PERLIN, M., and CECCIO, S.L. (2012) *On the energy economics of air lubrication drag reduction*. International Journal of Naval Architecture and Ocean Engineering, 4, 412-422.
- MAKIHARJU, S.A., ELBING, B.R., WIGGINGS, A., SHINASI, S., VANDENBROECK, J.-M., PERLIN, M., DOWLING, D.R., and CECCIO, S.L. (2013) *On the scaling of air entrainment from a ventilated partial cavity*. Journal of Fluid Mechanics, 732, 47-76.
- MATVEEV, K.I. (2003) *On the limiting parameters of artificial cavitation*. Ocean Engineering, 30(9), 1179-1190.
- MATVEEV, K.I. (2005) *Application of artificial cavitation for reducing ship drag*. Oceanic Engineering International, 9(1), 35-41.
- MATVEEV, K.I., DUNCAN, R., and WINKLER, J. (2006) *Acoustic, dynamic, and hydrodynamic aspects of air-lubricated hulls*. Undersea Defence Technology Conference, San Diego, California, USA.
- MATVEEV, K.I. and OCKFEN, A. (2009) *Modelling of hard-chine hulls in transitional and early planing regimes by hydrodynamic point sources*. International Shipbuilding Progress, 56(1-2), 1-13.
- MATVEEV, K.I., BURNETT, T., and OCKFEN, A. (2009) *Study of air-ventilated cavity under model hull on water surface*. Ocean Engineering, 36(12-13), 930-940.
- MATVEEV, K.I. (2014) *Modeling of finite-span ram wings moving above water at finite Froude numbers*. Journal of Ship Research, 58(3), 146-156.
- MATVEEV, K.I. (2015) *Hydrodynamic modeling of semi-planing hulls with air cavities*. International Journal of Naval Architecture and Ocean Engineering, 7(3), 500-508.
- SHIRI, A., LEER-ANDERSEN, M., BENSOW, R.E., and NORRBY, J. (2012) *Hydrodynamics of a displacement air cavity ship*. 29th Symposium on Naval Hydrodynamics, Gothenburg, Sweden.

24. ZVERKHOVSKYI, O., VAN TERWISGA, T., GUNSING, M., WESTERWEEL, J., and DELFOS, R. (2014) *Experimental study on drag reduction by air cavities on a ship model*. 30th Symposium on Naval Hydrodynamics, Hobart, Tasmania, Australia.